ORIGINAL RESEARCH

In Vivo Demonstration of Neuroinflammatory Molecule Expression in Brain Abscess with Diffusion Tensor Imaging

R.K. Gupta
K. Nath
A. Prasad
K.N. Prasad
M. Husain
R.K.S. Rathore
N. Husain
C. Srivastava
P. Khetan
R. Trivedi
P.A. Narayana

BACKGROUND AND PURPOSE: Neuroinflammatory molecules, including tumor necrosis factor-α, interleukin1-β, lymphocyte function associated molecule-1, and intercellular cell adhesion molecule-1 contribute to the development of brain abscess. We hypothesized that the high fractional anisotropy (FA) in the brain abscess cavity reflects the upregulation of these neuroinflammatory molecules.

MATERIALS AND METHODS: Diffusion tensor imaging (DTI) was performed in 24 patients with brain abscess and *Staphylococcus aureus*–treated as well as nontreated Jurket cell lines (at 4 time points: 1, 24, 48, and 72 hours). Neuroinflammatory molecules were quantified from the brain abscess cavity aspirate of the patients as well as from the heat-killed *S aureus*–treated and nontreated cell lines and correlated with DTI measures.

RESULTS: The DTI-derived FA strongly correlated with the presence of neuroinflammatory molecules in the pus as well as in *S aureus*–treated cell lines; no such correlation was observed in nontreated cell lines.

CONCLUSIONS: These data indicate that neuroinflammatory molecules confer high diffusion anisotropy inside the brain abscess cavity. We propose that increased FA reflects upregulated inflammatory response in brain abscess.

Despite significant advances in the diagnosis and treatment, brain abscess remains a potentially fatal central nervous system infection. Brain abscess develops in response to a parenchymal infection by bacteria, beginning as a localized area of cerebritis and evolving into a suppurative lesion surrounded by a well-vascularized fibrotic capsule. The leading etiologic agents of brain abscess are the *Streptococcus* species and *Staphylococcus aureus*, though a myriad of other organisms have also been implicated.[1,2] Animal models also implicate proinflammatory molecules such as tumor necrosis factor-alpha (TNF-α) and interleukin1-beta (*IL1-*β) in the development of brain abscess.[3] These proinflammatory molecules, in turn, induce various cell adhesion molecules (CAMs), including selectins, intercellular cell adhesion molecules (*ICAM-1*), vascular cell adhesion molecules, and platelet-endothelial cell adhesion molecules. These CAMs facilitate the extravasation of peripheral immune cells, perpetuating the antibacterial immune response that is thought to contribute, at least in part, to the development of brain abscess.[4,5] Consistent with this mechanistic model, analysis of various neuroinflammatory molecules (NMs) shows an initial marked enhancement, persistence, and subsequent depletion with time in animal models of brain abscess.[5-8] Some of these findings have been reproduced in human brain cells, for example, TNF-α and *IL1-*β induce *ICAM-1* expression in human brain endothelial cells.[6-8]

Diffusion tensor imaging (DTI) is a relatively new MR imaging technique that has been shown to provide tissue microstructural information.[9] The commonly used DTI-derived metrics are fractional anisotropy (FA) and mean diffusivity (MD). Organized structures such as white matter tracts are characterized by high FA values. However, recently high FA in the brain abscess cavity has been reported.[10] We hypothesized that the high FA in the brain abscess cavity reflects the upregulation of various adhesion molecules on inflammatory cells, which confers the structured orientation of these cells in the abscess cavity. In the current study, for the first time, we demonstrate a correlation between FA, as measured by in vivo DTI, and various NMs in the brain abscess cavity aspirate from 24 patients. We have also confirmed these observations through ex vivo assays, in which we have induced NMs in Jurket cell lines by exposing them to heat-killed *S aureus*. The results of these studies may have significant clinical implications and could provide a noninvasive way of detecting active inflammation in vivo.

Methods

Study Design

Twenty-four patients with brain abscess (16 males and 8 females; median age, 28 years; range, 1–50 years) were consecutively studied. MR imaging, including DTI, was performed on all these patients. Institutional ethics approval and informed consent from all the patients or their nearest kin were obtained. Patients with an initial diag-

Received May 4, 2007; accepted after revision August 9.

From the Departments of Radiodiagnosis (R.K.G., K.N., R.T.) and Microbiology (A.P., K.N.P.), Sanjay Gandhi Post Graduate Institute of Medical Sciences, Lucknow, UP, India; Departments of Neurosurgery (M.H., C.S., P.K.) and Pathology (N.H.), King George's Medical University, Lucknow, UP, India; Department of Mathematics and Statistics (R.K.S.R.), Indian Institute of Technology, Kanpur, UP, India; and Department of Diagnostic and Interventional Imaging (P.A.N.), University of Texas Medical School at Houston, Houston, Tex.

This work was supported by the Indian Council of Medical Research (Grant No. 5/4–5/12/Neuro/2005-NCD-I) and Life Sciences Research Board-Defence Research and Development Organization (DLS/81/48222/LSRB-129/ID/2007), New Delhi, India. Kavindra Nath, Amit Prasad, and Richa Trivedi acknowledge the financial assistance from the Indian Council of Medical Research, University Grants Commission, and Council of Scientific and Industrial Research, New Delhi, India, respectively.

Paper previously presented in part at: Fourteenth Scientific Meeting of International Society for Magnetic Resonance in Medicine, May 6–12, 2006; Seattle, Wash.

Please address correspondence to Rakesh K. Gupta, MD, MR Section, Department of Radiodiagnosis, Sanjay Gandhi Post Graduate Institute of Medical Sciences, Lucknow, UP, India-226014; e-mail: rgupta@sgpgi.ac.in

Indicates article with supplemental on-line tables

DOI 10.3174/ajnr.A0826

nosis of brain abscess, based on conventional MR imaging, including diffusion imaging as well as in vivo proton MR spectroscopy, were selected. The diagnosis of brain abscess was finally confirmed at surgery and by the results of the culture of the aspirated pus.

The following predisposing factors were recognized in 13 patients: otitis media ($n = 8$), dental caries ($n = 2$), congenital heart disease ($n = 1$), postmeningitis ($n = 1$), and postoperative infection ($n = 1$). In the remaining 11 patients, the cause of infection could not be ascertained. Sonography-guided aspiration of the pus was performed in all the patients. Following aspiration, part of the pus was inoculated in BACTEC Plus Aerobic and Anaerobic media (Becton, Dickinson and Company, Sparks, Md), and the remainder was preserved at −70°C for the quantitation of various NMs.

Culture of Pus

Immediately after aspiration from the abscess cavity, pus was inoculated into BACTEC aerobic and anaerobic culture bottles and incubated at 37°C, and growth was monitored every day for 5 days. Media with positive growth were subcultured on appropriate solid media. Aerobic incubation was carried out at 37°C for 24 hours, and anaerobic incubation was carried out in jars filled with the gas mixture of nitrogen (80%–90%), carbon dioxide (CO_2) (5%–10%), and hydrogen (5%–10%) through an anoxomat system (Mart BV Microbiology, Lichtenvoorde, Holland). All the isolates were identified by standard biochemical tests as described previously.[11] The causative microorganisms confirmed after culture were aerobic *Streptococci* sp. (n = 6), *S aureus* ($n = 5$), *Streptococcus uberis* ($n = 3$), *Bacteroides* sp. ($n = 2$), *Nocardia* species ($n = 2$), *Pseudomonas aeruginosa* ($n = 1$), and sterile ($n = 2$) and mixed microbes (aerobic and anaerobic) ($n = 3$).

Cell Line

The Jurket cell line (clone E6–1), a T-cell line (lymphocytic origin) having a nonadherent property (floating in nature), was subjected to ex vivo studies to validate our in vivo results. It was cultured in Roswell Park Memorial Institute-1640 medium supplemented with 10% fetal calf serum, 2.0-mmol/L L-glutamine, 1.5-g/L sodium bicarbonate, 4.5-g/L glucose, 10-mmol/L HEPES (Sigma-Aldrich, St. Louis, Mo), and 1.0-mmol/L sodium pyruvate. The cells were grown in 24 (T-75) different flasks (12 experimental and 12 controls). Twelve flasks were treated with heat-killed (94.5°C for 10 minutes) *S aureus* (ATCC 25923) and further incubated in a CO_2 incubator. The cell count ratio of heat-killed *S aureus* and Jurket cell lines was 1:100. MR imaging of heat-killed *S aureus*–treated as well as nontreated cell lines was performed at 4 time points: 1, 24, 48, and 72 hours. The photomicrographs (×10) of heat-killed *S aureus*–treated as well as nontreated cell lines at each time point (1, 24, 48, and 72 hours) were taken using Eclipse (TE 2000-S, Nikon, Melville, NY).

MR Imaging Protocol in Patients

Conventional MR images and DTI images were acquired on a 1.5T MR imaging scanner (GE Healthcare, Milwaukee, Wis) by using a standard quadrature birdcage receive and transmit radio-frequency head coil. The conventional MR imaging protocol included T2-weighted fast spin-echo (SE) images with TR/TE/echo-train length/NEX = 6000/85/16/4 and SE T1-weighted images with TR/TE/NEX = 1000/14/2. Both T1-weighted and T2-weighted images were acquired from contiguous (interleaved) 3-mm-thick axial sections with 240 × 240 mm FOV and an image matrix of 256 × 256. Postcontrast T1-weighted images were acquired after intravenous injection of gadopentate dimeglumine (Gd-DTPA-BMA, Omniscan; Amersham Health, Oslo, Norway) at a dose of 0.1 mmol/kg of body weight.

DTI data were acquired by using a single-shot echo-planar dual SE sequence with ramp sampling.[12] A balanced[13] rotationally invariant[14,15] dodecahedral diffusion-gradient encoding scheme with 10 uniformly distributed directions over the unit hemisphere was used. The b factor was 1000 s/mm^2. The acquisition parameters were the following: section thickness of 3 mm with no gap, number of sections = 34–38, FOV = 240 × 240 mm, TR = 8 sec, TE = 100 ms, and NEX = 8. The acquisition matrix was 128 × 80, and the homodyne algorithm was used to construct the *k*-space data to 128 × 128 and zero-filled to generate an image matrix of 256 × 256.

MR Imaging Protocol in Cell Lines

The DTI acquisition parameters were the following: b factor = 1000 s/mm^2, section thickness of 3 mm with no gap, number of sections = 10, FOV = 100 × 100 mm, TR = 8 sec, TE = 100 ms, and NEX = 14. The acquisition matrix of 128 × 128 followed by zero-filling to generate an image matrix of 256 × 256 was used. For DTI at each time point (1, 24, 48, and 72 hours), the cells were pooled from 3 flasks and harvested by centrifugation. A total of 4×10^7 cells were taken at each time point for experimentation. To provide better signal intensity-to-noise ratio, we added 0.5% gadodiamide (Gd-DTPA-BMA; Omniscan, Amersham Health, Oslo, Norway) in phosphate buffer saline (PBS) to the cell line.[16] We imaged 0.5 mL of sample (including the cell line and Gd-DTPA-BMA in PBS) in a 0.5-mL microcentifuge tube at each time point. The microcentifuge tube was embedded in a big plastic container filled with 2% agarose gel and taken for DTI imaging. The total imaging time for the DTI experiment was 19.36 minutes. From the same pool of cells, 1×10^6 cells were snap frozen for molecular quantification, the same as the pus sample.

DTI Data Processing and Quantitation

The DTI data were processed as described elsewhere.[13] Briefly, following image cropping and distortion corrections, the data were interpolated to attain isotropic voxels and decoded to obtain the tensor field for each voxel. The eigenvalues (λ_1, λ_2, and λ_3) and the 3 orthonormal eigenvectors were determined. The eigenvalues were used to compute the FA for each voxel.

To calculate the FA in the brain abscess cavity, we performed an automated segmentation by using the in-house developed JAVA-based software. The facilitated region-of-interest encircling the whole lesion was drawn, and the lesion was automatically segmented into the 2 subregions with FA < 0.20 and FA ≥ 0.20. FA values obtained from the abscess cavity having FA > 0.20 were used for the statistical correlation with NMs. This threshold was chosen because major white matter tracts are seen at the 0.2-FA cutoff in normal brain parenchyma.[10] For the region-of-interest placement for quantitative analysis, the DTI-derived maps were displayed and overlaid on images with different contrasts in the 3 orthogonal planes for a visual inspection. FA values were calculated by placing the region of interest in the brain abscess cavity of all the sections showing the lesion.

The DTI data of nontreated as well as heat-killed *S aureus*–treated cell lines were processed and analyzed at each time point by using the same procedure as in patients except for the size of the regions of interest. The size of the region of interest was typically 2 × 2 pixels, with shape varying from elliptical to freehand drawing. For the FA quantitation at each time point, 4–6 sections in which the cell line was

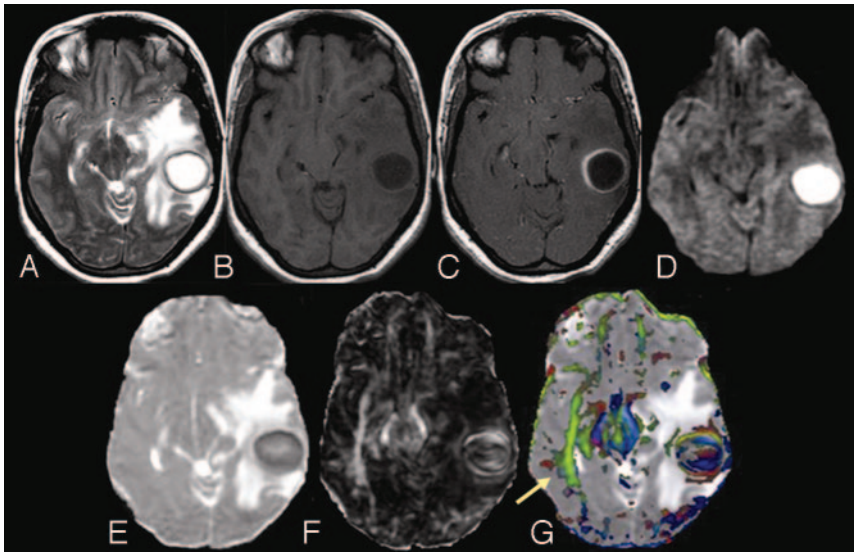

Fig 1. A 31-year-old female patient presenting with pyogenic brain abscess in the left temporal lobe. *A,* Axial T2-weighted image shows a well-defined hyperintense lesion with a hypointense wall. *B,* The lesion appears hypointense on the axial T1-weighted image with an isointense wall. *C,* On the postcontrast T1-weighted image, the lesion shows ring enhancement. *D,* DWI shows homogeneous hyperintensity in the cavity that appears hypointense on the MD map (*E*). The FA (*F*) and red-green-blue color-modulated FA map fused with the MD map (*G*) show that high FA in the abscess cavity is similar to what is observed in the contralateral inferior longitudinal fasciculus and midbrain (*arrow*).

best visualized were selected. In all the cases with brain abscess, FA values were calculated by selecting the cutoff value of 0.20.[10]

Ribonucleic Acid Isolation and Reverse Transcriptase-Polymerase Chain Reaction

The NMs quantified through reverse transcriptase-polymerase chain reaction (RT-PCR) from the pus of the brain abscess cavity of patients and cell lines were IL1-β, lymphocyte function associated molecule-1 (LFA-1), and TNF-α and will be referred to as NMs in the remainder of the article. Total ribonucleic acid (RNA) was extracted from the pus collected during surgery as well as from the cell line at different time points (1, 24, 48, 72 hours) by using RNeasy Kit (Qiagen, Valencia, Calif) according to the manufacturer's instructions. Complementary deoxyribonucleic acid (cDNA) was synthesized by RevertAid H Minus First Strand cDNA Synthesis Kit (Fermantas LIFE SCIENCES, Glen Burnie, Md) taking 100 ng of RNA for each sample. After reverse transcription, primer specific amplification of LFA-1 (CD11a), *IL1-* β, TNF-α, and glyceraldehyde-3-phosphate dehydrogenase (GAPDH) (housekeeping gene) was performed for the following specific primers: LFA-1 sense (5′-GAGCTCTTTGAGAACACCTC-3′), LFA-1 antisense (5′-TCACACTTCACTGTCACCTC-3′), TNF-α sense (5′CAGAGGGAAGAGTTCCCCAG-3′), TNF-α antisense (5′-CCTTGGTCTGGTAGGAGACG-3′), *IL1-*β sense (5′-AGATGAAGTGCTCCTTCCAG-3′), *IL1-*β antisense (5′-CAACACGCAGGACAGGTACAG−3′), and GAPDH sense (5′-GGTCGGAGTCAACGGATTTGGT-3′) and GAPDH antisense (5′-TGTGGGCC ATGAGGTCCACCAC-3′).

The size of products amplified by LFA-1, TNF-α, *IL1-*β, human soluble *ICAM-1* (sICam-1), and GAPDH primer pairs were 367, 427, 325, and 924 base pairs, respectively, in an MJ Research Cycler, PTC 100 (Perkin Elmer, Waltham, Mass). Following were the PCR cycles for amplification–primary denaturation at 95°C for 3′, followed by 94°C for 1′, annealing (52–58°C for 1′) and extension at 72°C for 1′ for 35 cycles, followed by final extension at 72°C for 5′. Amplified PCR products from pus as well as cell lines were detected by 2% agarose gel electrophoresis with 0.5-μg/mL ethidium bromide and photographed under ultraviolet illumination. Band intensities were quantified by densitometric scanning software, Image Ready Elite (Amersham Pharmacia Biotech, Uppsala, Sweden). To normalize messenger RNA levels, we scanned attenuation of LFA-1, TNF-α, *IL1-*β, and GAPDH bands from the same samples, and data were calculated as the ratios of band-intensity values of LFA-1, TNF-α, and *IL1-*β relative to the band intensity of GAPDH.

Quantitation of sICAM-1

Human sICAM-1 in pus was quantitatively measured by human sICAM-1 enzyme-linked immunosorbent assay (ELISA) (Cat. No. BBE1B, R&D Systems, Minneapolis, Minn). ELISA was performed as per the guidelines of the manufacturer. In brief, standard series/pus/cell culture supernatants were diluted 20 times in diluent buffer, and 100 μL of conjugate and sample was applied on each ELISA well. Incubated for 90 minutes, rigorously washed 6 times, 100 μL of substrate was added and again incubated for 30 minutes. Reaction was stopped by adding 100 μL of stop solution, and a reading was taken at 450 nm with wavelength correction at 620 nm (Sunrise ELISA Reader; Tecan, Salzburg, Austria). The amount of sICAM-1 in samples was determined by standard plot.

Statistical Analysis

Bivariate analysis of correlation was performed to study the relationship between the FA values in the brain abscess cavity and NMs extracted from pus, with the assumption that there was no correlation between DTI measures and NMs (Ho [null hypothesis] = 0). Alternatively, if a correlation >0.00 was observed at α = 0.05% and 90% power of test, the null hypothesis was rejected. The relationship between FA values in cell lines (heat-killed *S aureus*–treated and nontreated) and the NMs was also analyzed by using the same approach. The Pearson correlation coefficient was computed for each variable under study, with mean FA, MD, and NMs in both in vivo and ex vivo studies. Sample size estimation was performed by using Power and Sample Size (PASS 6.0; Dynalab Test Systems, Reynoldsburg, Ohio), and other statistical computations were performed by using the Statistical Package for Social Sciences, Version 12.0 (SPSS, Chicago, Ill) statistical software.

Results

Brain abscesses were located in the frontal lobe (n = 1), parietal lobe (n = 6), temporal lobe (n = 2), occipital lobe (n = 2), frontoparietal region (n = 3), temporoparietal region (n = 1), temporo-occipital region (n = 2), parieto-occipital region (n = 2), and cerebellum (n = 5). The brain abscess appeared hyperintense on T2-weighted images with a peripheral hy-

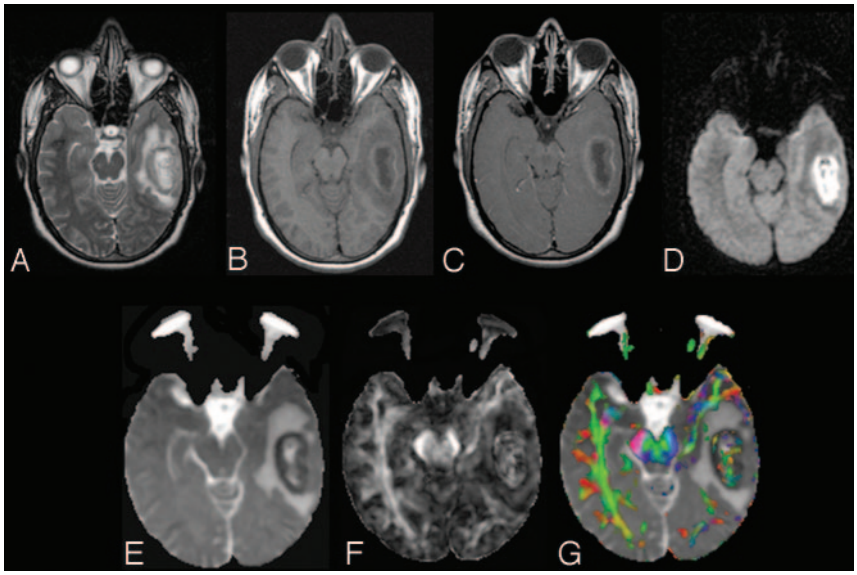

Fig 2. A 25-year-old male patient presenting with pyogenic brain abscess with a heterogeneously hyperintense lesion in the left temporal lobe. *A*, Axial T2-weighted image shows a hyperintense lesion with a hypointense wall. *B*, The lesion appears hypointense on the axial T1-weighted image with an isointense wall. *C*, On the postcontrast T1-weighted image, the lesion shows ring enhancement. *D*, The lesion appears heterogeneously hyperintense on the DWI in the cavity that appears heterogeneously hypointense on the MD map (*E*). The FA (*F*) and red-green-blue color-modulated FA map fused with MD map (*G*) show that high FA in the abscess cavity is similar to what is observed in the contralateral inferior longitudinal fasciculus and midbrain.

pointense rim (Fig 1*A*) and iso- to hypointense on T1-weighted images (Fig 1*B*). On postcontrast T1-weighted images, brain abscess showed rim enhancement (Fig 1*C*). On diffusion-weighted images (DWI), we observed 2 types of signal-intensity distribution: 1) homogeneously hyperintense, when the signal intensity of the lesion was homogeneously high in the abscess cavity (Fig 1); and 2) heterogeneously hyperintense, when the lesion contained both high and low signal intensities intermixed in variable proportions in the abscess cavity (Fig 2). Among the 24 patients with brain abscess, 10 brain abscesses appeared homogeneously hyperintense and the remaining 14 were heterogeneously hyperintense on DWI images.

The mean FA and MD values in the subregion of the brain abscess cavity having FA $>$0.20 were 0.25 $\pm$ 0.07 and (0.74 $\pm$ 0.23) $\times$ 10^{-3} mm^2/s, respectively. In subregions having FA $<$0.20, mean FA and MD values were 0.12 $\pm$ 0.04 and (0.64 $\pm$ 0.18) $\times$ 10^{-3} mm^2/s, respectively. The mean band-intensity ratios of NMs quantified through RT-PCR from the pus of brain abscess cavities of patients were the following: *IL1-β*/GAPDH, LFA-1/GAPDH, and TNF-α/GAPDH = 2.52 $\pm$ 0.96, 2.48 $\pm$ 1.19, and 2.37 $\pm$ 0.92, respectively. The sICAM-1 quantified through ELISA was 94.97 $\pm$ 46.38. Significant positive correlations between FA and NMs (Fig 3*A*, -*B*) and among NMs were found.

FA values of nontreated as well as heat-killed *S aureus*–treated cell lines at different time points (1, 24, 48, 72 hours) are summarized in supplemental on-line Table 1. The FA value was significantly higher in the heat-killed *S aureus*–treated cell line at 24, 48 and 72 hours (Fig 4*A*), compared with the nontreated cell line of same group (Fig 4*B*). The band-intensity ratios of *IL1-β*/GAPDH, LFA-1/GAPDH, TNF-α/GAPDH, and sICAM-1 in heat-killed *S aureus*–treated as well as nontreated cell lines are summarized in supplemental on-line Table 1. LFA-1 did not show quantifiable expression in nontreated cell lines at 1 and 24 hours (Fig 4*C*).

Significant positive correlations between FA and NMs and among NMs were found at each time point in the heat-killed *S aureus*–treated cell lines except in case of sICAM-1 at 1 hour (supplemental on-line Table 2) (Fig 3*C*–*F*). In nontreated cell lines, significant positive correlation was found between FA, *IL1-β*/GAPDH, and TNF-α/GAPDH at 1 hour only. Among NMs, significant positive correlation was found between *IL1-β*/GAPDH and TNF-α/GAPDH at 0, 48, and 72 hours.

On photomicrographs (Fig 5), an increased degree of cell aggregation in the heat-killed *S aureus*–treated cell line was observed subsequently with time compared with the nontreated cell line.

Discussion

Various cell adhesion molecules in the aggregation of inflammatory cells have been postulated to be responsible for the high FA in the brain abscess cavity.[10] In this study, we have shown the possible mechanism of high FA in the brain abscess cavity through the in vivo and ex vivo studies. Significant positive correlation between FA and various NMs quantified from aspirated brain abscess pus suggests the role of these NMs for increased FA inside the cavity. The in vivo observations were further confirmed by the ex vivo DTI of both nontreated and *S aureus*–treated Jurket cell lines incubated with heat-killed *S aureus* (ATCC 25923). The heat-killed *S aureus*–treated cell lines showed a pattern of results similar to those obtained in vivo in the brain abscess cavity and showed similar correlation with NMs. We preferred to use heat-killed rather than live bacteria to avoid the cytolytic effect.[17] It has been shown that the intact bacteria generate the same inflammatory response as the cell wall components (peptidoglycan and lipopolysaccharide) of the bacteria and independently activate the chemokines in human monocytes.[18]

There is growing evidence of increase in NM expression at the site of inflammation with in vivo as well as ex vivo studies.[19,20] On blocking experiments with anti-*ICAM*-1 and anti-LFA-1 antibodies, authors have demonstrated leukocytic aggregation of inflammatory cells mediated via *ICAM-1* and LFA-1 interaction.[20] We did not find any correlation between FA and NMs in the nontreated cell lines (Fig 2*C*–*F*), except for significant positive correlation at 1 hour between FA, *IL1-β*/GAPDH, and TNF-α/GAPDH; however significant positive correlation between FA and NMs in the heat-killed *S aureus*–treated cell lines at each time point was observed. Our obser-

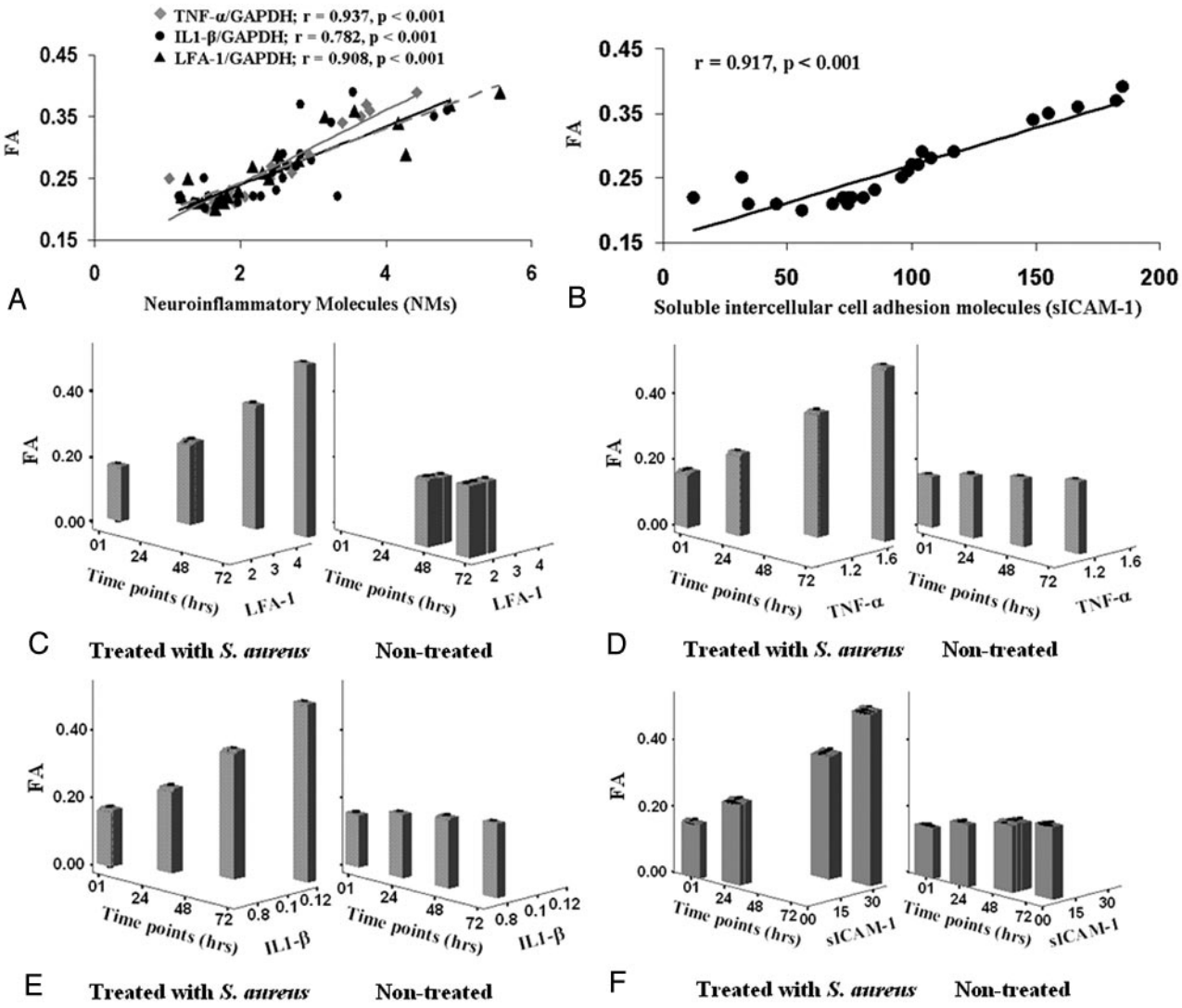

Fig 3. *A*, Plots showing the relationship (*A*) between FA and *IL1-β*, TNF-α, and LFA-1. *B*, FA and sICAM-1 in pus from the abscess cavity. *C–F*, The relationship between FA and NMs in heat-killed *S aureus*–treated as well as nontreated cell lines at different time points (1, 24, 48, and 72 hours [hrs]) is depicted in the form of bar plots.

vation of NMs expression in the nontreated cell lines at 1 hour is consistent with a previous study demonstrating baseline expression of NMs in controls at 40 minutes.[18] FA values and NM expression at 1 hour can be considered as baseline values because no significant change in FA values and expression of NMs was observed in the nontreated cell lines subsequently with time. Significant positive correlation between FA and NMs at each time point in the heat-killed *S aureus*–treated cell lines suggests that these NMs are upregulated in response to the infection and further confirms the mechanism behind increased FA in brain abscess cavity.

In both ex vivo and in vivo studies, no correlation between MD values and NMs was observed. Brain abscess is usually associated with high signal intensity on DWI with reduced MD values.[21] The viable inflammatory cells and bacteria have been thought to be responsible for restricted diffusion in brain abscess.[22] MD values reflect change in cell attenuation and extracellular space.[23] In nontreated cell lines, no significant changes in MD values were observed with time because of the insignificant change in the number of cells taken for imaging at each time point. However, the heat-killed *S aureus*–treated cell lines showed an increasing pattern of MD values with time with significant decrease in cells at each time point. This may be due to the increased proportion of dead cells relative to the viable cells with time, resulting in an increased extracellular space with a concomitant increase in MD. An association between treatment response and increased MD values in the brain abscess cavity has been reported previously.[24] However, the current ex vivo studies suggest that increased FA with minimal increase in MD with time are associated with increased NMs and may be a more specific and robust marker of inflammatory response. In both ex vivo and in vivo studies, no correlation between FA and MD value was observed at any time point. Our observations are in line with the previous DTI study in patients with brain abscess, which showed a large variation in FA values with no significant changes in MD values.[10]

We observed high FA in the brain abscess cavity in 2 patients who had no bacterial growth on pus culture (sterile). It suggests that remnants of bacterial cell walls are responsible for the continued release of NMs, even when the pus from the abscess cavity may not yield any bacterial growth on culture. It

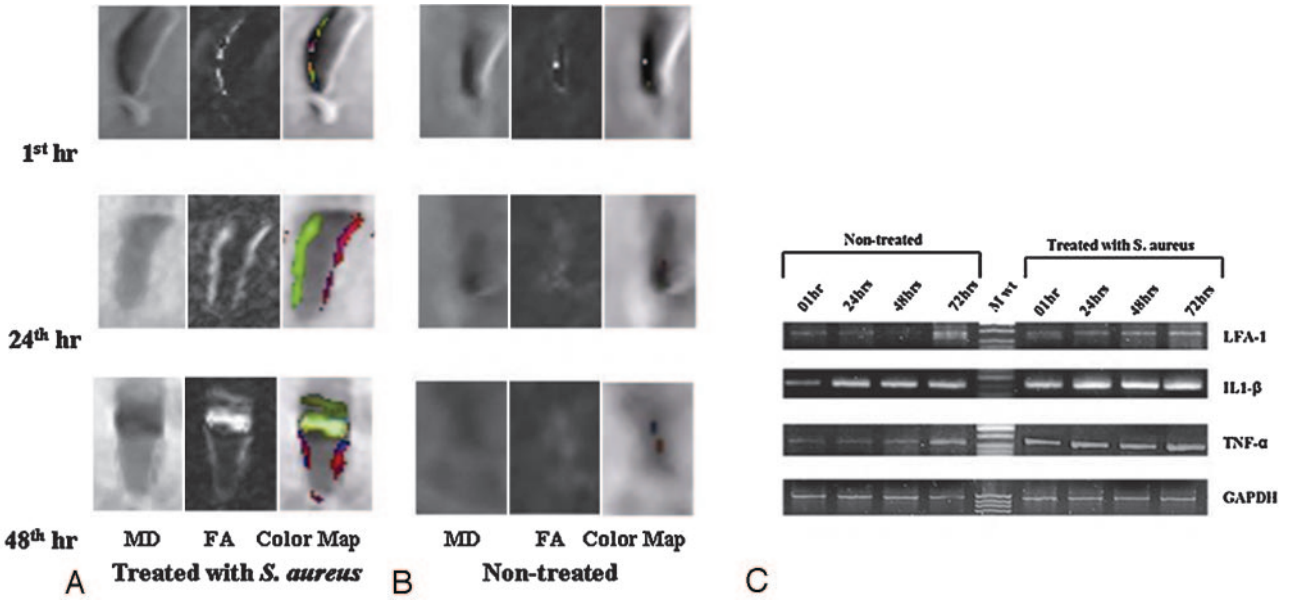

Fig 4. *A*, Coronal images of MD, FA, and color-coded FA maps fused with MD of Jurket cell lines treated with heat-killed *S aureus* at 1, 24, and 48 hours (hr), respectively, show an increase in FA and MD. *B*, The corresponding maps for nontreated Jurket cells show very few changes in FA and MD. *C*, Expression of LFA-1, *IL1-β*, TNF-α, and GAPDH (housekeeping) genes in nontreated and heat-killed *S aureus*–treated Jurket cell lines at 1, 24, 48, and 72 hours.

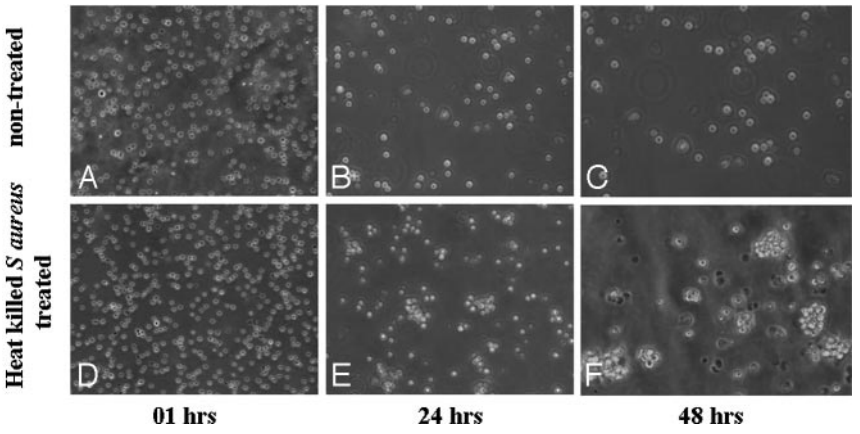

Fig 5. Cell aggregation at different time points in nontreated (*A–C*) and heat-killed *S aureus*–treated (*D–F*) cell lines. Photomicrographs of heat-killed *S aureus*–treated cell line with a time course show an increased degree of cell aggregation compared with that in nontreated cell line. hrs indicates hours.

has been shown in a brain abscess animal model that the number of inflammatory cells does not decrease significantly even if the abscesses show a marked decrease in bacterial colony count in culture with time.[19] This has been shown to be due to continuous release of proinflammatory cytokines and chemokines even after a decreased bacterial load. Continued release of NMs by activated glia and infiltrating peripheral immune cells may cause damage to surrounding brain parenchyma, which is responsible for long-term neurologic consequences, including seizures and cognitive deficits in patients with brain abscess.[1] The demonstration of the continued increase in FA in patients who are on therapy may suggest continued activity of the disease process and may require specific anti-inflammatory intervention to control this activity. This may reduce the posttreatment sequelae, like seizures and cognitive decline, in the future.

In other inflammatory pathologies such as multiple sclerosis (MS) and meningitis, the role of various NMs has also been reported. The role of *ICAM-1*, -2, and LFA-1 in the transendothelial migration of leukocytes into MS brain and the role of *ICAM-3*/LFA-1 interaction in the activation of lymphocytes, monocytes, and microglia in MS lesions have already been reported.[25] Although the mechanism is unknown, it has been suggested that the NMs play a major role in the leukocyte aggregation in meningitis.[26] Significantly increased leukocyte aggregation score and expression of sICAM-1 and L-selectins have been reported in the CSF of pediatric patients with bacterial meningitis compared with patients with viral meningitis.[27] Serum procalcitonin and C-reactive proteins have been used as diagnostic markers of inflammation in sepsis.[28] These markers may also be raised in a variety of nonspecific inflammations. Detection of inflammatory markers from CSF and serum in bacterial meningitis and MS is an indirect approach to seeing an inflammatory response that may be responsible for contradictory conclusions.[29-33] In vivo detection of activity of NMs at the lesion site may help in more precise assessment of the ac-

tivity of the disease and thus may be helpful in clinical management of these patients.

Conclusion

Because FA shows a strong correlation with all NMs at the site of infection, we propose that increased FA in brain abscess reflects upregulation of various adhesion molecules on inflammatory cells at the site of the local infective process.

Acknowledgment

We thank Dr. C. M. Pandey, Department of Biostatistics, Sanjay Gandhi Post Graduate Institute of Medical Sciences, Lucknow, India, for his support in statistical analysis.

References

1. Mathisen GE, Johnson JP. **Brain abscess.** *Clin Infect Dis* 1997;25:763–92
2. Townsend GC, Scheld WM. **Infections of the central nervous system.** *Adv Internal Med* 1998;43:403–47
3. Kielian T. **Immunopathogenesis of brain abscess.** *J Neuroinflammation* 2004;17:1–16
4. Kielian T. **Microglia and chemokines in infectious diseases of the nervous system: views and reviews.** *Front Biosci* 2004;9:732–50
5. Kielian T, Bearden ED, Baldwin AC. **IL-1 and TNF-alpha play a pivotal role in the host immune response in a mouse model of Staphylococcus aureus-induced experimental brain abscess.** *J Neuropathol Exp Neurol* 2004;63:381–96
6. Wong D, Dorovini-Zis K. **Upregulation of intercellular adhesion molecule-1 (ICAM-1) expression in primary cultures of human brain microvessel endothelial cells by cytokines and lipopolysaccharide.** *J Neuroimmunol* 1992;39:11–21
7. Vassalli P. **The pathophysiology of tumor necrosis factors.** *Annu Rev Immunol* 1992;10:411–528
8. Bevilacqua MP. **Endothelial-leukocyte adhesion molecules.** *Annu Rev Immunol* 1993;11:767–804
9. Mori S, Zhang J. **Principles of diffusion tensor imaging and its application to basic neuroscience research.** *Neuron* 2006;51:527–39
10. Gupta RK, Hasan KM, Mishra AM, et al. **High fractional anisotropy in brain abscesses versus other cystic intracranial lesions.** *AJNR Am J Neuroradiol* 2005;26:1107–14
11. Prasad KN, Mishra AM, Gupta D, et al. **Analysis of microbial etiology and mortality in patients with brain abscess.** *J Infect* 2006;53:221–27
12. Basser PJ. **Inferring microstructural features and the physiological state of tissues from diffusion-weighted images.** *NMR Biomed* 1995;8:333–44
13. Hasan KM, Parker DL, Alexander AL. **Comparison of gradient encoding schemes for diffusion-tensor MRI.** *J Magn Reson Imaging* 2001;13:769–80
14. Batchelor PG, Atkinson D, Hill DL, et al. **Anisotropic noise propagation in diffusion tensor MRI sampling schemes.** *Magn Reson Med* 2003;49:1143–51
15. Hasan KM, Narayana PA. **Computation of the fractional anisotropy and mean diffusivity maps without tensor decoding and diagonalization: theoretical analysis and validation**. *Magn Reson Med* 2003;50:589–98
16. Zhang Z, van den Bos EJ, Wielopolski PA, et al. **High-resolution magnetic resonance imaging of iron-labeled myoblasts using a standard 1.5-T clinical scanner.** *MAGMA* 2004;17:201–09
17. Segura M, Stankova J, Gottschalk M. **Heat-killed Streptococcus suis capsular type 2 strains stimulate tumor necrosis factor alpha and interleukin-6 production by murine macrophages.** *Infect Immun* 1999;67:4646–54
18. Wang ZM, Liu C, Dziarski R. **Chemokines are the main proinflammatory mediators in human monocytes activated by Staphylococcus aureus, peptidoglycan, and endotoxin.** *J Biol Chem* 2000;275:20260–67
19. Baldwin AC, Kielian T. **Persistent immune activation associated with a mouse model of Staphylococcus aureus-induced experimental brain abscess.** *J Neuroimmunol* 2004;151:24–32
20. Moese S, Selbach M, Meyer TF, et al. **Cag+ Helicobacter pylori induces homotypic aggregation of macrophage-like cells by up-regulation and recruitment of intracellular adhesion molecule 1 to the cell surface.** *Infect Immun* 2002;70:4687–91
21. Mishra AM, Gupta RK, Jaggi RS, et al. **Role of diffusion-weighted imaging and *in vivo* proton magnetic resonance spectroscopy in the differential diagnosis of ring-enhancing intracranial cystic mass lesions.** *J Comput Assist Tomogr* 2004;28:540–47
22. Mishra AM, Gupta RK, Saksena S, et al. **Biological correlates of diffusivity in brain abscess.** *Magn Reson Med* 2005;54:878–85
23. Le Bihan D. **Looking into the functional architecture of the brain with diffusion MRI.** *Nat Rev Neurosci* 2003;4:469–80
24. Cartes-Zumelzu FW, Stavrou I, Castillo M, et al. **Diffusion-weighted imaging in the assessment of brain abscesses therapy.** *AJNR Am J Neuroradiol* 2004;25:1310–17
25. Bo L, Peterson JW, Mork S, et al. **Distribution of immunoglobulin superfamily members ICAM-1, -2, -3, and the beta 2 integrin LFA-1 in multiple sclerosis lesions.** *J Neuropathol Exp Neurol* 1996;55:1060–72
26. Garty BZ, Berliner S, Liberman E, et al. **Cerebrospinal fluid leukocyte aggregation in meningitis.** *Pediatr Infect Dis J* 1997;16:647–51
27. Uysal G, Tulek N, Ozhan B. **Leukocyte aggregation score in meningitis and its relationship with cerebrospinal fluid soluble selectin and soluble ICAM-1 levels.** *J Trop Pediatr* 2000;46:381–82
28. Castelli GP, Pognani C, Cita M, et al. **Procalcitonin, C-reactive protein, white blood cells and SOFA score in ICU: diagnosis and monitoring of sepsis.** *Minerva Anestesiol* 2006;72:69–80
29. Meisner M, Tschaikowsky K, Palmaers T, et al. **Comparison of procalcitonin (PCT) and C-reactive protein (CRP) plasma concentrations at different SOFA scores during the course of sepsis and MODS.** *Crit Care* 1999;3:45–55
30. Ugarte H, Silva E, Mercan D, et al. **Procalcitonin used as a marker of infection in the intensive care unit.** *Crit Care Med* 1999;27:498–504
31. Muller B, Becker KL, Schachinger H, et al. **Calcitonin precursors are reliable markers of sepsis in a medical intensive care unit.** *Crit Care Med* 2000;28:977–83
32. Luzzani A, Polati E, Dorizzi R, et al. **Comparison of procalcitonin and C-reactive protein as markers of sepsis.** *Crit care Med* 2003;31:1737–41
33. Chan YL, Tseng CP, Tsay PK, et al. **Procalcitonin as a marker of bacterial infection in the emergency department: an observational study.** *Crit Care* 2004;8:R12–20